



Short-lived radionuclides in presolar SiC grains: constraints on timescales in AGB stars

A. M. Davis¹ and R. Gallino²

¹ Chicago Center for Cosmochemistry, Enrico Fermi Institute, University of Chicago, and Department of the Geophysical Sciences, Chicago, IL 60637 USA e-mail: a-davis@uchicago.edu

² Dipartimento di Fisica Generale dell'Università di Torino and INFN, Sezione di Torino, Via P. Giuria 1, I-10125 Torino, Italy

Abstract. Presolar grains from asymptotic giant branch (AGB) stars preserve evidence of the decay of short-lived radionuclides. We review evidence for the former presence of such nuclides and their implications for AGB timescales.

Key words. Asymptotic giant branch stars, Presolar grains, Extinct radionuclides

1. Introduction

Since their discovery in the late 1980s (Lewis et al. 1987; Bernatowicz et al. 1987; Amari et al. 1990), presolar grains have gained prominence as recorders of physical and nucleosynthetic conditions in stars. Stellar evolution and nucleosynthesis modeling are often considered to be mature fields in astrophysics. However, since presolar grains directly sample stars, they provide opportunities to test models in ways that have not previously been possible.

In this paper, we focus on the most widely studied type of presolar grain, silicon carbide (SiC), and on the most common type of SiC, mainstream grains, which are believed to grow in the outflows of low-mass, carbon-rich AGB stars. For current reviews of presolar grains, see Zinner (2003), Clayton & Nittler (2004) and Lugaro (2005). A number of radionuclides with half-lives much shorter than the age of the solar system are produced in AGB stars and

evidence of their decay is preserved in presolar SiC. We review here evidence for the former presence of such nuclides, compare the inferred amounts with nucleosynthesis calculations and explore the implications of short-lived nuclides for AGB timescales.

2. Short-lived radionuclides produced in AGB stars

The main component of the *s*-process occurs in the helium intershell of thermally pulsing low-mass AGB stars. Two neutron sources operate in these stars: $^{13}\text{C}(\alpha, n)^{16}\text{O}$, which provides a low flux exposure for thousands of years in the ^{13}C pocket during interpulse periods; and $^{22}\text{Ne}(\alpha, n)^{25}\text{Mg}$, which provides a high flux exposure for only a few years during thermal pulses (Gallino et al. 1998; Lugaro et al. 2003).

Table 1 contains a complete list of short-lived radionuclides produced in AGB stars. In the column labeled “Amount”, we normalize to a stable isotope and give the ratio in the

Table 1. Short-lived radionuclides produced in low-mass AGB stars, with the amount present in the envelope after the last thermal pulse with third dredge-up in a $2 M_{\odot}$ AGB star of initially solar metallicity

Parent	Daughter	Half-life (My)	Amount	Comment
^{26}Al	^{26}Mg	0.717	$^{26}\text{Al}/^{27}\text{Al}=3.9 \times 10^{-3}$	detected in SiC, oxides
^{36}Cl	$^{36}\text{S}, ^{36}\text{Ar}$	0.301	$^{36}\text{Cl}/^{35}\text{Cl}=4.7 \times 10^{-4}$	volatile parent
^{41}Ca	^{41}K	0.103	$^{41}\text{Ca}/^{40}\text{Ca}=2.6 \times 10^{-5}$	detected in oxides
^{60}Fe	^{60}Ni	1.5	$^{60}\text{Fe}/^{56}\text{Fe}=3.1 \times 10^{-6}$	worth looking for in silicates
^{79}Se	^{79}Br	0.65	$^{79}\text{Se}/^{76}\text{Se}=1.1 \times 10^{-4}$	volatile parent
^{81}Kr	^{81}Br	0.229	$^{81}\text{Kr}/^{82}\text{Kr}=6.3 \times 10^{-3}$	volatile parent
^{93}Zr	^{93}Nb	1.53	$^{93}\text{Zr}/^{90}\text{Zr}=0.20$	detected in SiC
^{99}Tc	^{99}Ru	0.211	$^{99}\text{Tc}/^{99}\text{Ru}=0.18$	detected in SiC
^{107}Pd	^{107}Ag	6.5	$^{107}\text{Pd}/^{108}\text{Pd}=0.13$	worth looking for in SiC
^{135}Cs	^{135}Ba	2.3	$^{135}\text{Cs}/^{133}\text{Cs}=0.23$	detected in SiC
^{146}Sm	^{142}Nd	103	$^{146}\text{Sm}/^{144}\text{Sm}=1.8 \times 10^{-3}$	low abundance; low Sm/Nd in SiC
^{182}Hf	^{182}W	9	$^{182}\text{Hf}/^{180}\text{Hf}=7.4 \times 10^{-3}$	worth looking for in SiC
^{205}Pb	^{205}Tl	15.3	$^{205}\text{Pb}/^{204}\text{Pb}=0.93$	volatile parent

envelope of a $2 M_{\odot}$ AGB star of initially solar metallicity after the last thermal pulse with third dredge-up. In the models considered here, the amount of ^{13}C present in the pocket is a free parameter, and in Table 1 we give results for the “standard” case, which provides a good match to heavy element isotopic patterns in mainstream SiC grains (Lugaro et al. 2003; Barzyk et al. 2006). The normalizing isotope used is either an abundant *s*-process isotope or the isotope most commonly used for normalization in the cosmochemistry literature.

3. Unfavorable cases

For several of the short-lived radionuclides listed in Table 1, both the parent and daughter isotope are volatile elements that cannot condense at the high temperatures at which known types of presolar grains form in stellar outflows, so evidence is unlikely to be found in presolar grains. The nuclides in this group are ^{36}Cl , ^{79}Se , ^{81}Kr and ^{205}Pb .

^{60}Fe is also unfavorable. Although trace element abundance measurements show significant amounts of iron and nickel in presolar SiC, Fe/Ni ratios are approximately one tenth the solar system ratio (Kashiv 2004), so that the expected variations in $^{60}\text{Ni}/^{58}\text{Ni}$ are an-

anticipated to be much less than 1 permil and would be overwhelmed by *s*-process variations in this ratio. ^{60}Fe is made by neutron capture on ^{58}Fe and ^{59}Fe during the $^{22}\text{Ne}(\alpha, n)^{25}\text{Mg}$ exposure during thermal pulses and is insensitive to the amount of ^{13}C present in the ^{13}C pocket. Recent models, in which an *s*-process nucleosynthesis network calculation is integrated into an AGB stellar evolution code, suggest levels of ^{60}Fe that are as much as a factor ten higher (Cristallo et al. 2006), but the effect would still be difficult to detect in presolar SiC. Iron-bearing presolar silicates with AGB signatures in their oxygen isotopes have been found in primitive meteorites (Nguyen & Zinner 2004). Presolar olivine, $(\text{Mg,Fe})_2\text{SiO}_4$, and pyroxene, $(\text{Mg,Fe})\text{SiO}_3$, have both been reported. In meteorites, both phases can have high Fe/Ni ratios, so presolar silicates might be a promising place to look for evidence of extinct ^{60}Fe when techniques are developed to measure nickel isotopes on submicron grains.

^{146}Sm is primarily a *p*-process isotope, but it can be produced in small quantities by neutron capture on the initial *p*-process ^{144}Sm present in AGB stars. The amount listed in Table 1 is about one-third the early solar system $^{146}\text{Sm}/^{144}\text{Sm}$ ratio (McKeegan & Davis 2003). Since any AGB contribution to the early

solar system amount of ^{146}Sm must have been significantly diluted by other material, AGB stars cannot be major contributors to the early solar system ratio. ^{146}Sm would only be detectable in mainstream presolar SiC if there was some chemical fractionation that enhanced the Sm/Nd ratio. However, recent measurements of trace element abundances in SiC-bearing diamond aggregates show that SiC has low Sm/Nd ratios compared to ratios predicted by the *s*-process (Yin et al. 2005), (Ott et al. 2006). This indicates that samarium is more volatile than neodymium under conditions appropriate for SiC condensation in AGB stars.

4. Light elements: ^{26}Al and ^{41}Ca

Presolar SiC grains have $^{25}\text{Mg}/^{24}\text{Mg}$ ratios that are solar to within $\sim 10\%$, but $^{26}\text{Mg}/^{24}\text{Mg}$ ratios that can be greatly in excess of solar, especially when the Al/Mg ratio is high. The $^{26}\text{Al}/^{27}\text{Al}$ ratio at the time of SiC grain formation can be calculated from the magnesium isotopic composition and Al/Mg ratio. In mainstream SiC grains with clear ^{26}Mg excesses, $^{26}\text{Al}/^{27}\text{Al}$ ratios are typically in the range of 10^{-4} to 10^{-3} (Hoppe et al. 1994) but can be as high as $\sim 10^{-2}$ (Zinner 1998). Levels as high as $\sim 10^{-3}$ can be explained by normal AGB models, mostly via $^{25}\text{Mg}(p, \gamma)^{26}\text{Al}$ at the base of the convective envelope, but special mechanisms, such as cool-bottom processing, must be appealed to to explain higher ratios (Nollett et al. 2003).

Excess ^{41}K has been reported in hibonite, CaAl_2O_9 , grains from AGB stars (Nittler et al. 2005), but not in mainstream SiC grains. Calcium-41 is made by neutron capture on ^{40}Ca during the $^{22}\text{Ne}(\alpha, n)^{25}\text{Mg}$ exposure during thermal pulses and is insensitive to the amount of ^{13}C present in the ^{13}C pocket.

5. ^{93}Zr

^{93}Zr is along the main path of the *s*-process, because its half-life is long enough that it behaves as if it were stable in the *s*-process. ^{93}Zr decays to monoisotopic ^{93}Nb , so at first glance this might not be considered as a good case to look for enrichments in the daughter isotope. However, most ^{93}Nb is made as ^{93}Zr .

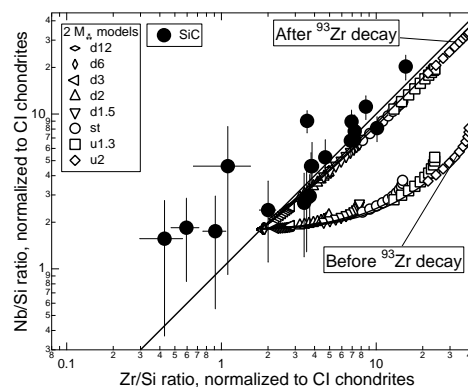


Fig. 1. Zirconium and niobium abundances in presolar SiC grains, which are Zr/Si and Nb/Si ratios normalized to solar system values. Two sets of AGB models are plotted, giving predicted compositions before and after ^{93}Zr decay.

In Fig. 1, we compare recent measurements of zirconium and niobium concentrations in presolar SiC by synchrotron x-ray fluorescence with nucleosynthesis calculations. The comparison shows clear evidence for in situ decay of ^{93}Zr in presolar grains (Kashiv et al. 2006). In the calculations, we explore the full plausible range of ^{13}C pocket amounts, from one-twelfth (d12) to twice (u2) the amount in the standard case (st). If no ^{93}Zr had been made in AGB stars, the data would lie along the trajectories labeled "Before ^{93}Zr decay". Instead the data tend to lie along trajectories labeled "After ^{93}Zr decay". Some of the data lie to the left of the latter trajectories. ZrC is more refractory than SiC. Kashiv et al. (2006) have suggested that ZrC may have been removed from the cooling gas in AGB winds by condensation prior to formation of SiC. The points to the left of the AGB predictions could be explained by various degrees of prior removal of ZrC, as long as niobium fully condenses into SiC.

6. ^{99}Tc

Like ^{93}Zr , ^{99}Tc is along the main path of the *s*-process and has a half-life that is long enough that it behaves as if it were stable. The half-life is only a few times longer than the typical interpulse time in AGB stars, a

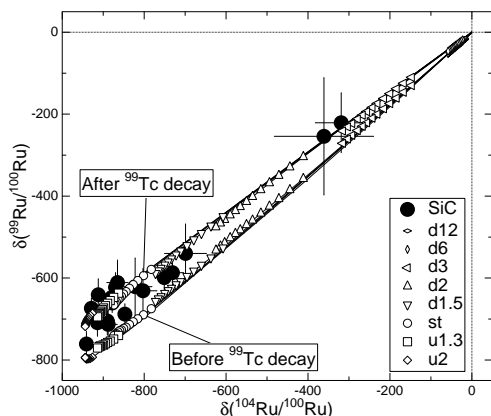


Fig. 2. Ruthenium isotopic compositions in single presolar SiC grains. ^{100}Ru is *s*-only, ^{104}Ru is *r*-only and ^{99}Ru is about 3/4 *r*-process. Models are shown for a $2 M_{\odot}$ AGB star of initially solar metallicity. Two cases are shown: before and after ^{99}Tc , under the assumption that both technetium and ruthenium fully condense into each grain.

few tens of thousands of years, so a significant amount of ^{99}Tc decays to ^{99}Ru during the AGB phase. Nonetheless, the comparison of ruthenium isotopic compositions of individual presolar SiC grains with nucleosynthesis calculations in Fig. 2 clearly shows that these grains had live ^{99}Tc in them when they formed (Savina et al. 2004). The data match the curve labeled “After ^{99}Tc decay” much better than the one labeled “Before ^{99}Tc decay”. The neutron capture cross sections for this system are well-known and the discrepancy between the data and the curve labeled “Before ^{99}Tc decay” is outside the uncertainties due to cross sections (Savina et al. 2004).

The inferred presence of technetium in presolar grains is especially important, as it ties the grains to the red giant stars in which technetium was found by spectroscopic techniques more than 50 years ago (Merrill 1952; Savina et al. 2004).

7. ^{135}Cs

The main path of the *s*-process does not pass through ^{135}Cs , but there is a branch point at ^{134}Cs . This isotope has a half-life of 2.06 y, so

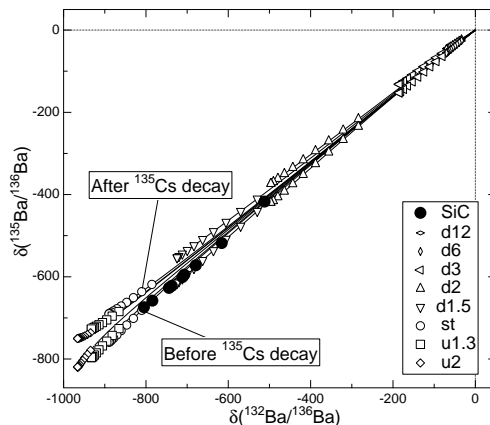


Fig. 3. Barium isotopic compositions in aggregates of presolar SiC from the Murchison (Ott & Begemann 1990; Prombo et al. 1993) and Indarch (Jennings et al. 2002) meteorites. ^{136}Ba is *s*-only, ^{132}Ba is *p*-only and ^{135}Ba is mostly *r*-process. Models are shown for a $2 M_{\odot}$ AGB star of initially solar metallicity. Two cases are shown: for before and after decay of ^{135}Cs .

there is a significant branch toward the neutron capture channel during thermal pulses. High precision isotopic measurements made on aggregates of SiC are plotted in Fig. 3, along with AGB predictions. It can be seen that the data match predictions well if SiC condenses before ^{135}Cs decays, but less well if SiC condenses after ^{135}Cs decays (Lugaro et al. 2003). Cesium is a volatile element and barium is refractory, so only barium will condense into SiC. ^{135}Cs must have been live when the mainstream SiC grains condensed.

8. Other nuclides worth looking for

Two other short-lived radionuclides listed in Table 1 have the potential of leaving a record of their decay in mainstream presolar SiC grains.

^{107}Pd is produced in fairly high abundance in AGB stars (Fig. 4), as it is on the main path of the *s*-process and has a half-life long enough that it behaves as if it were stable. Palladium is not usually thought of as an element with a stable refractory carbide, but measurements of trace element abundances in the SiC-bearing diamond aggregate studied by Yin et al. (2005)

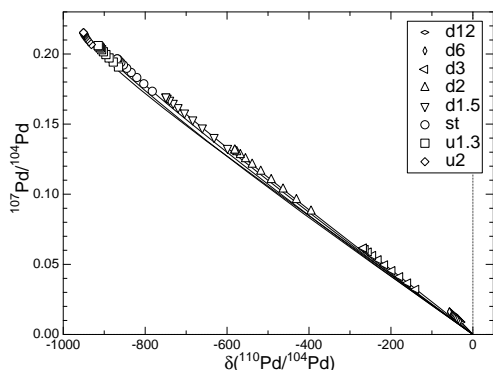


Fig. 4. $^{107}\text{Pd}/^{104}\text{Pd}$ ratios vs. $\delta(^{110}\text{Pd}/^{104}\text{Pd})$, the deviation from the solar $^{110}\text{Pd}/^{104}\text{Pd}$ ratio in parts per thousand. ^{110}Pd is r -only and ^{104}Pd is s -only. Models are shown for a $2 M_{\odot}$ AGB star of initially solar metallicity.

reveal a significant concentration of palladium (Ott et al. 2006). As silver is a fairly volatile element, mainstream SiC grains may have fairly high $^{107}\text{Ag}/^{109}\text{Ag}$ ratios.

^{182}Hf is not on the main path of the s -process, but can be made via the neutron capture channel at the ^{181}Hf ($T_{1/2}=42$ d) branch point. Both hafnium and tungsten have refractory carbides. If both elements fully condense into SiC, shifts in $\delta(^{182}\text{W}/^{184}\text{W})$ of up to 13 and 38 permil are to be expected for 2 (Fig. 5) and 3 M_{\odot} solar metallicity models, respectively. Some enhancement in Hf/W ratios due to chemistry would make this search more favorable.

9. Implications for AGB timescales

The production rates of the heavy short-lived radionuclides ^{93}Zr , ^{99}Tc , and ^{135}Cs are well-constrained in AGB nucleosynthesis calculations. Stellar evolution codes for low-mass AGB stars indicate interpulse periods of a few tens of thousands of years, interspersed with thermal pulses of a few years (e.g., Lattanzio & Boothroyd 1997). These timescales are not in conflict with those inferred from isotopic evidence for the decay of extinct radionuclides. While not surprising, this gives added confidence in the models. Grain condensation in AGB outflows is believed to occur on

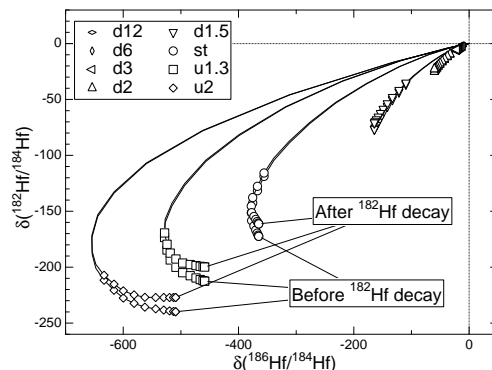


Fig. 5. $\delta(^{182}\text{W}/^{184}\text{W})$ vs. $\delta(^{186}\text{Hf}/^{184}\text{Hf})$. ^{186}W is r -only and ^{184}W has the largest s -contribution of the tungsten isotopes. Assuming both hafnium and tungsten fully condense into SiC, ^{182}Hf decay only shifts $\delta(^{182}\text{W}/^{184}\text{W})$ by a few permil. Models are shown for a $2 M_{\odot}$ AGB star of initially solar metallicity.

timescales of years or less. The grain data for barium indicate condensation before decay of ^{135}Cs , not very constraining, but also reassuring.

Acknowledgements. This work was supported by the U. S. National Aeronautics and Space Administration, through a grant to AMD. RG acknowledges support by the Italian MIUR-FIRB project “Astrophysical origin of elements beyond the Fe peak”.

References

- Amari, S., Anders, E., Virag, A., & Zinner, E. 1990, *Nature*, 345, 238
- Barzyk, J. G., Savina, M. R., Davis, A. M., et al. 2006, *New Astron. Rev.*, in press
- Bernatowicz, T. J., Fraundorf, G., et al. 1987, *Nature*, 330, 728
- Clayton, D. D. & Nittler, L. R. 2004, *ARA&A*, 42, 39
- Cristallo, S., Gallino, R., et al. 2006, *MemSAIT*, this issue
- Gallino, R., et al. 1998, *ApJ*, 497, 388
- Hoppe, P., Amari, S., Zinner, E., Ireland, T., & Lewis, R. S. 1994, *ApJ*, 430, 870
- Jennings, C. L., et al. 2002, *Lunar Planet. Sci.*, 33, #1833

- Kashiv, Y. 2004, Ph.D. dissertation, University of Chicago
- Kashiv, Y., et al. 2006, *Lunar Planet. Sci.*, 37, #2464
- Lattanzio, J. C. et al. AIP Conf. Proc. 402, Amer. Inst. Phys., New York, 85
- Lewis, R. S., Ming, T., Wacker, J. F., & Anders, E. 1987, *Nature*, 326, 160
- Lugaro, M. 2005, *Stardust from Meteorites: an Introduction to Presolar Grains*, World Scientific, Singapore, 209 pp.
- Lugaro, M., et al. 2003, *ApJ*, 593, 486
- McKeegan, K. D. and Davis, A. M. *Treatise on Geochemistry*, Oxford: Elsevier-Pergamon, Vol. 1, 431
- Merrill, P. W. 1952, *ApJ*, 116, 21
- Nguyen, A. N. & Zinner, E. 2004, *Science*, 303, 1496
- Nittler, L. R., Alexander, C. M. O'D., Stadermann, F. J., & Zinner, E. 2005, *Lunar Planet. Sci.*, 36, #2200
- Nollett, K. M., Busso, M., & Wasserburg, G. J. 2003, *ApJ*, 582, 1036
- Ott, U., & Begemann, F. 1990, *ApJ*, 353, L57
- Ott, U., Yin, Q.-Z., & Lee, C.-T. 2006, *MemSAIT*, 77, 890
- Prombo, C. A., Podosek, F. A., Amari, S., & Lewis, R. S. 1993, *ApJ*, 410, 393
- Savina, M. R., et al. S. 2004, *Science*, 303, 649
- Yin, Q.-Z., Ott, U., & Lee, C. T. 2005, *Meteorit. Planet. Sci.*, 40, A143
- Zinner, E. 1998, *ARA&A*, 26, 147
- Zinner, E. K. 2003, in *Meteorites, Comets, and Planets*, ed. Davis, A. M., *Treatise on Geochemistry*, Oxford: Elsevier-Pergamon, Vol. 1, 17